

Supporting Information

Synthesis of Bi_2Te_3 and $(\text{Bi}_x\text{Sb}_{1-x})_2\text{Te}_3$ Nanoparticles using the novel IL $[\text{C}_4\text{mim}]_3[\text{Bi}_3\text{I}_{12}]$.

Manuel Loor, Georg Bendt, Ulrich Hagemann, Christoph Wölper, Wilfried Assenmacher,
Stephan Schulz*

Content

Fig. S1-S3. ^1H and ^{13}C NMR spectra; IR spectra of $[\text{C}_4\text{mim}]_3[\text{Bi}_3\text{I}_{12}]$ **1**.

Fig. S4. NMR spectroscopic study of the byproducts of the reaction of $(\text{Et}_3\text{Si})_2\text{Te}$ and $[\text{C}_4\text{mim}]_3[\text{Bi}_3\text{I}_{12}]$.

Fig. S5-S7. ^1H and ^{13}C NMR spectra; IR spectra of $[\text{C}_4\text{mim}]\text{I}$.

Fig. S8. Color change upon heating and cooling of $[\text{C}_4\text{mim}][\text{Bi}_3\text{I}_{12}]$ **1**.

Fig. S9. Temperature-dependent DSC study of **1**.

Table S1: Hydrogen bonds [\AA] and $^\circ$] for **1**.

Table S2: Inter-halide interactions [\AA and $^\circ$] for **1**.

Table S3: EDX results from STEM spot analyses on single crystals.

Fig. S1. ^1H -NMR spectrum of **1** in DMSO-d₆.

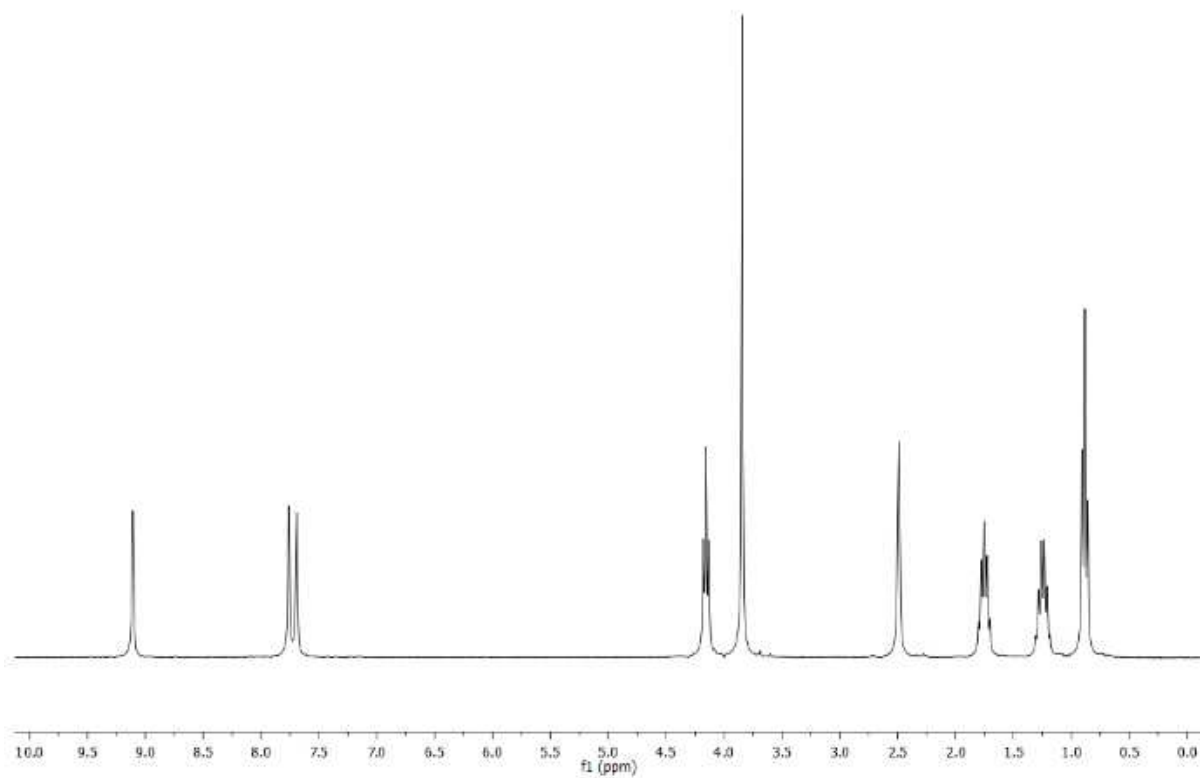


Fig. S2. ^{13}C -NMR spectrum of **1** in DMSO-d₆.

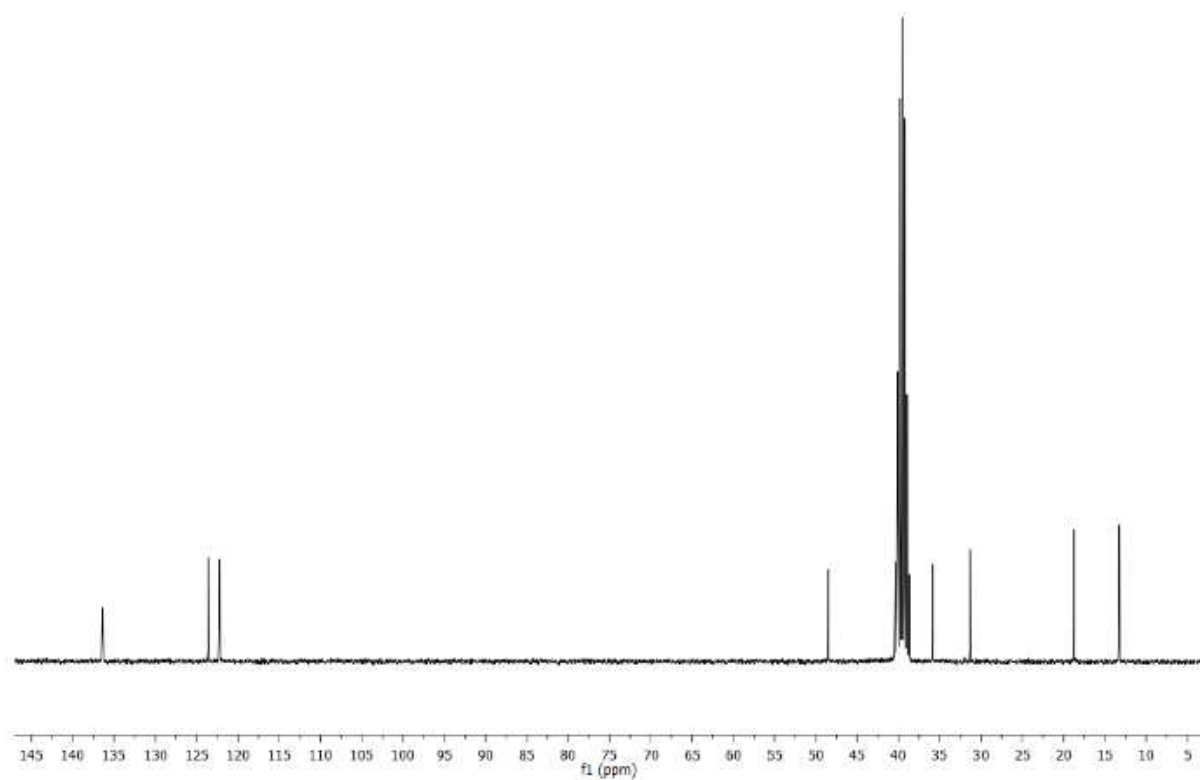


Fig. S3. IR absorption spectrum of **1**.

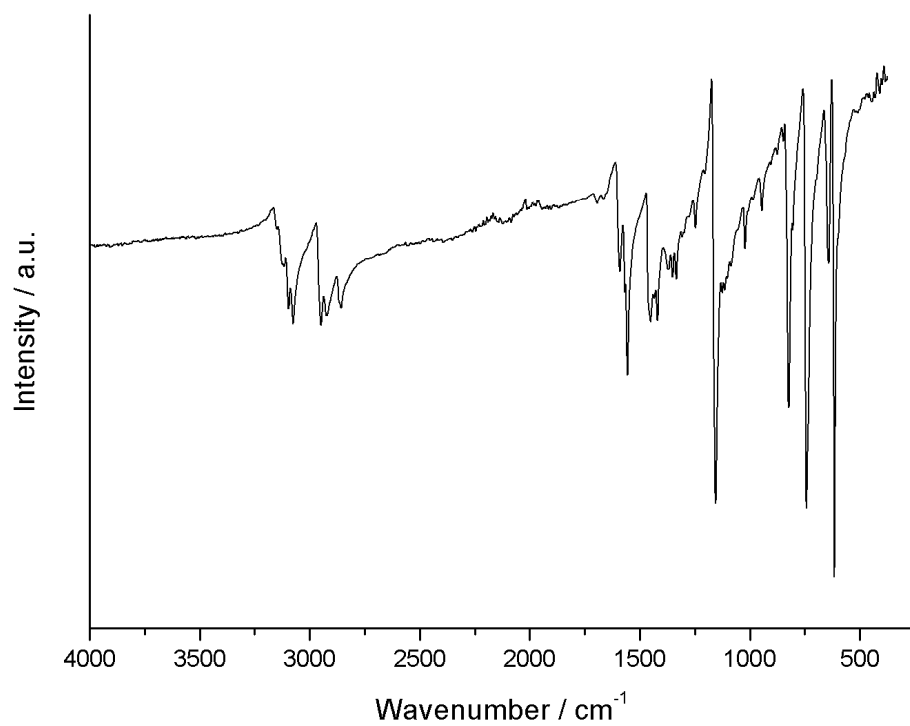


Fig. S4a. $^1\text{H-NMR}$ spectroscopic study in CDCl_3 of the byproducts of the reaction of $(\text{Et}_3\text{Si})_2\text{Te}$ and $[\text{C}_4\text{mim}]_3[\text{Bi}_3\text{I}_{12}]$; peaks marked with * correspond to Et_3SiI and those with # to Si_2Et_6 .

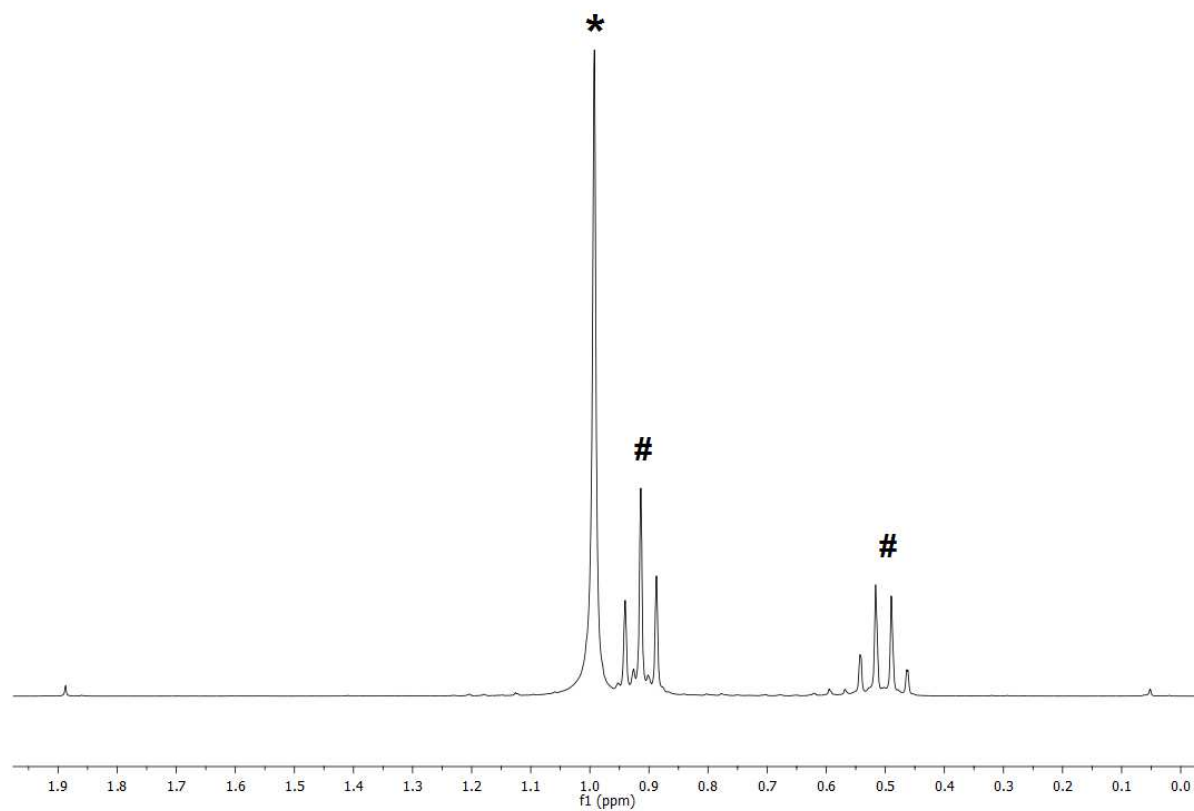


Fig. S4b. ^{13}C -NMR spectroscopic study in CDCl_3 of the byproducts of the reaction of $(\text{Et}_3\text{Si})_2\text{Te}$ and $[\text{C}_4\text{mim}]_3[\text{Bi}_3\text{I}_{12}]$; peaks marked with * correspond to Et_3SiI and those with # to Si_2Et_6 .

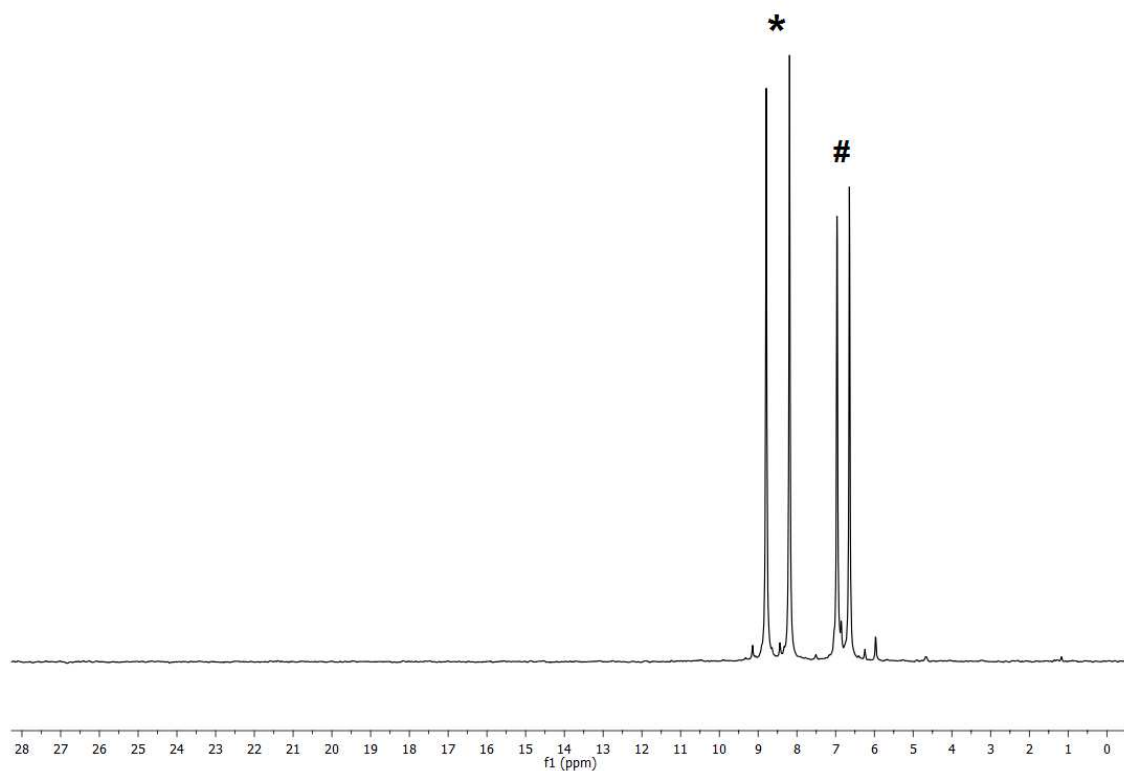


Fig. S4c. ^{29}Si -NMR spectroscopic study in CDCl_3 of the byproducts of the reaction of $(\text{Et}_3\text{Si})_2\text{Te}$ and $[\text{C}_4\text{mim}]_3[\text{Bi}_3\text{I}_{12}]$; peaks marked with * correspond to Et_3SiI and those with # to Si_2Et_6 .

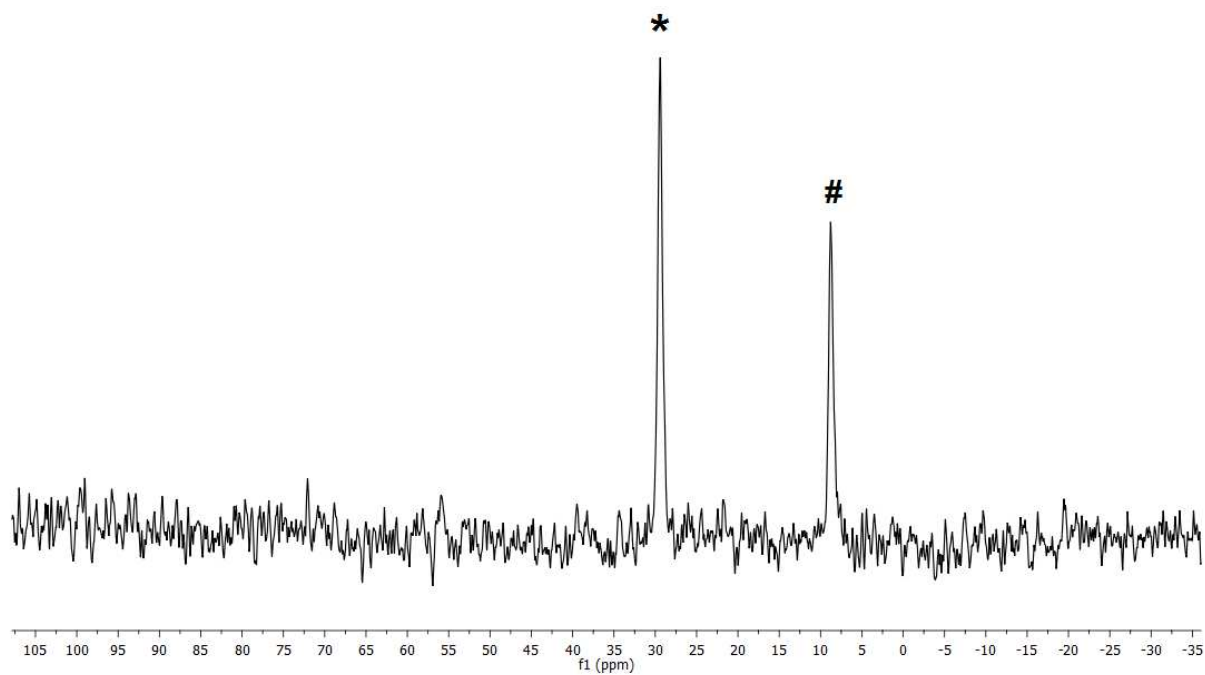


Fig. S5. ^1H -NMR spectrum of $[\text{C}_4\text{mim}][\text{I}]$ in DMSO-d_6 .

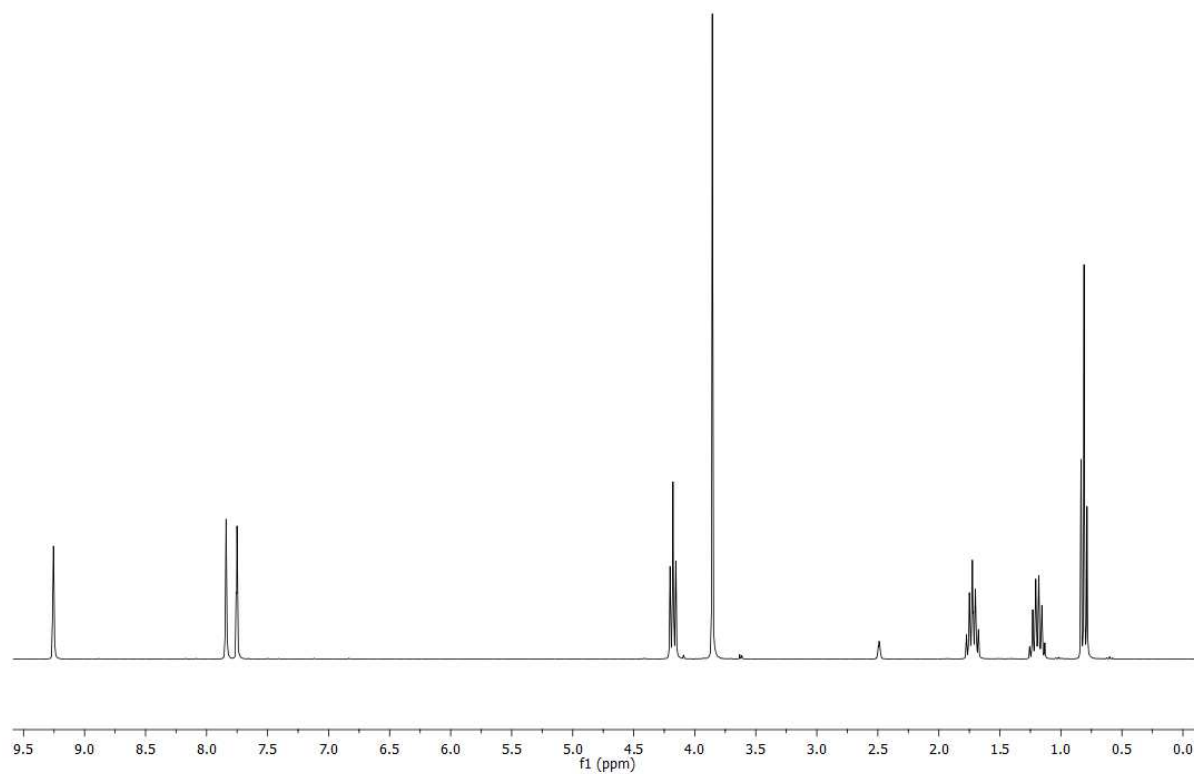


Fig. S6. ^{13}C -NMR spectrum of $[\text{C}_4\text{mim}][\text{I}]$ in DMSO-d_6 .

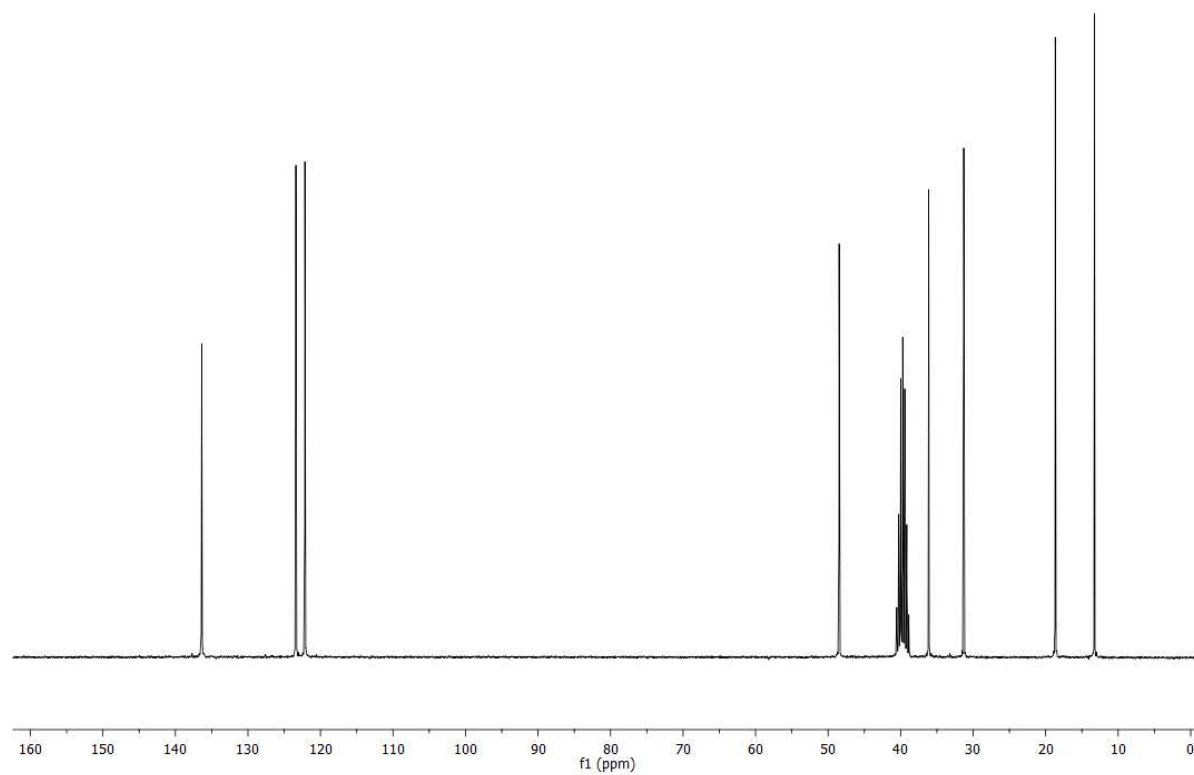


Fig. S7. IR-absorption spectrum of [C₄mim][I]

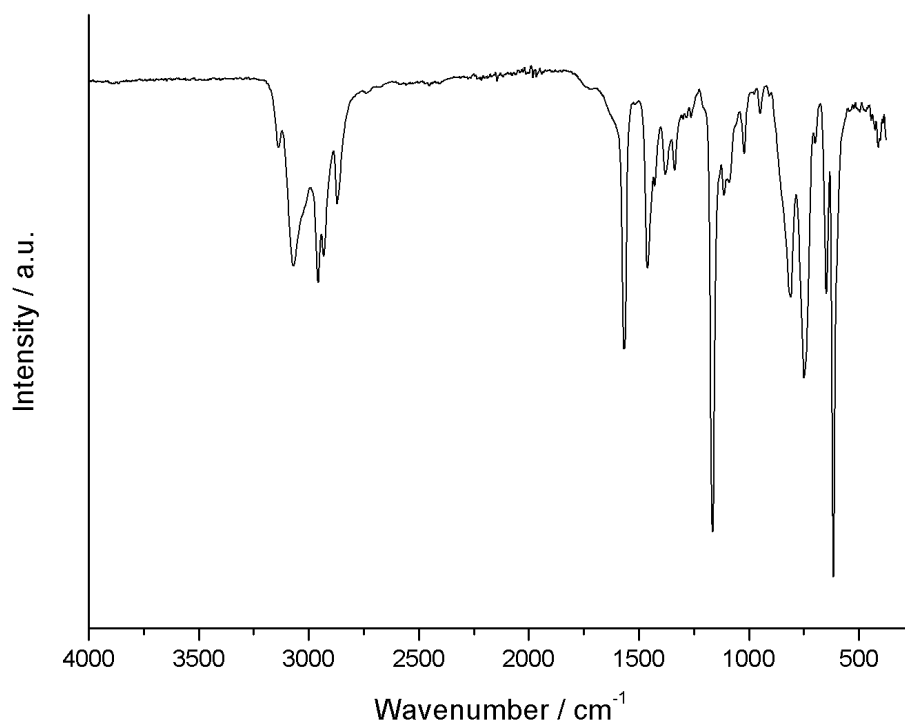


Fig. S8. Thermochromic behavior of **1**.

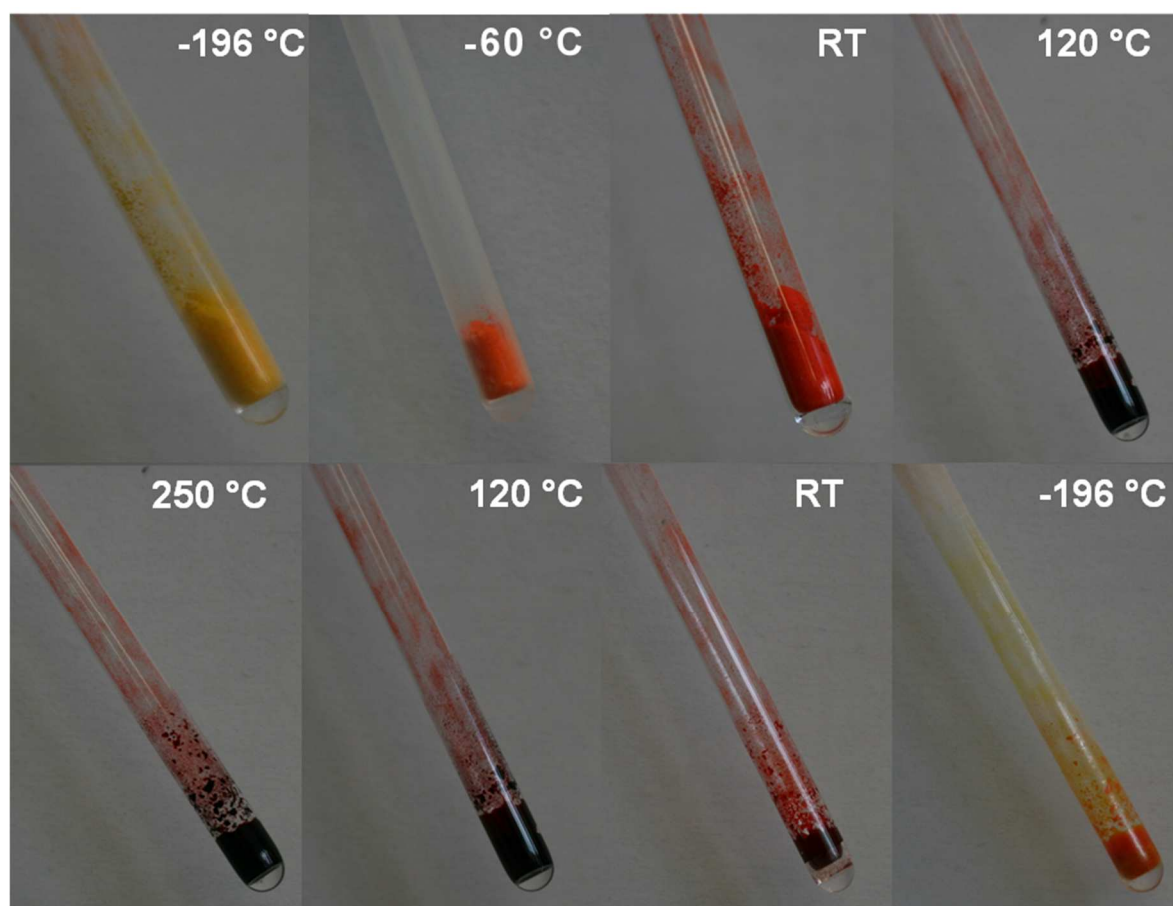


Fig. S9. Temperature-dependent DSC study of **1**.

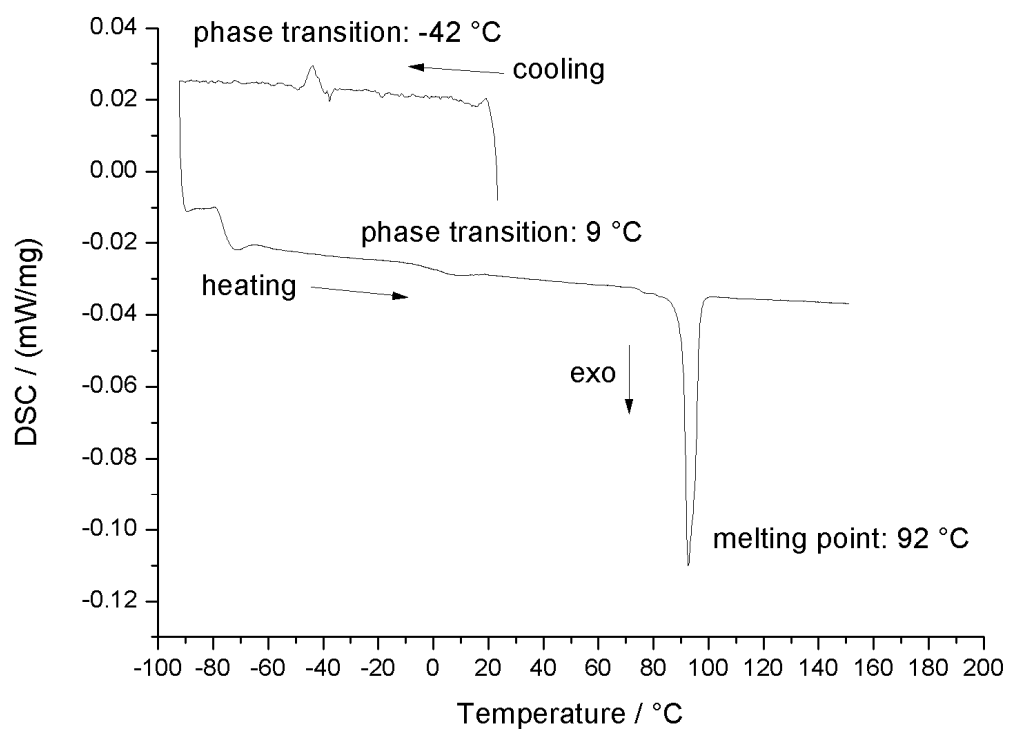


Table S1: Hydrogen bonds [\AA] and $^\circ$] for **1**.

D-H...A	d(D-H)	d(H...A)	d(D...A)	$\angle(\text{DHA})$
C(11)-H(11C)...I(13)	0.98	3.07	3.813(13)	133.7
C(13)-H(13)...I(23)#3	0.95	3.18	3.851(12)	129.3
C(13)-H(13)...I(24)	0.95	3.21	4.014(14)	143.5
C(16)-H(16A)...I(14)	0.99	3.26	4.089(12)	142.9
C(16)-H(16A)...I(16)	0.99	3.27	3.932(12)	126.1
C(21)-H(21A)...I(26)#3	0.98	3.27	4.035(13)	135.9
C(22)-H(22)...I(26)#3	0.95	3.09	3.929(12)	148.0
C(23)-H(23)...I(14)#4	0.95	3.13	3.981(13)	150.3
C(26)-H(26B)...I(24)#4	0.99	3.32	4.235(11)	153.7
C(31)-H(31A)...I(26)	0.98	3.28	4.168(15)	152.4
C(31)-H(31B)...I(16)#5	0.98	3.28	3.780(12)	113.3
C(31)-H(31C)...I(14)#4	0.98	3.31	4.167(13)	147.4
C(32)-H(32)...I(21)	0.95	3.23	3.928(13)	131.8
C(32)-H(32)...I(26)	0.95	3.11	3.860(12)	137.5
C(34)-H(34)...I(15)#6	0.95	3.29	4.128(13)	148.1
C(36)-H(36B)...I(16)#6	0.99	3.31	4.230(15)	155.4

#3 $x, -y+3/2, z+1/2$ #4 $-x+1, y-1/2, -z+1/2$ #5 $x+1, y, z$ #6 $x+1, -y+3/2, z-1/2$

Table S2: Inter-halide interactions [\AA] and $^\circ$] for **1**.

Bi-I...I-Bi	d(I...I)	$\angle(\text{Bi-I...I})$	$\angle(\text{I...I-Bi})$
Bi(12)-I(16)...I(11)#7-Bi(11)#7	3.8510(10)	152.58(2)	150.33(3)
Bi(12)-I(16)...I(11)#7-Bi(12)#7			97.76(2)
Bi(22)-I(24)...I(23)#3-Bi(22)#3	3.8778(10)	175.95(3)	144.51(3)
Bi(22)-I(24)...I(23)#3-Bi(21)#3			137.01(2)

#3 $x, -y+3/2, z+1/2$ #7 $-x, y-1/2, -z+1/2$

Table S3: EDX results from STEM spot analyses on single crystalsa) $(\text{Bi}_x\text{Sb}_{1-x})_2\text{Te}_3$ with $x = 0.25$

Philips/FEI CM300 UT FEG; 300 keV acc. Voltage; Thermo Noran NSS Ge-Detector

<i>Atom%</i>	<i>Sb-L</i>	<i>Te-L</i>	<i>Bi-L</i>	<i>esd</i>	<i>Sb-L</i>	<i>Te-L</i>	<i>Bi-L</i>
10(1)_pt1	26.11	60.68	13.22	10(1)_pt1	1.6	1.75	0.77
10(1)_pt2	26.23	65.88	7.89	10(1)_pt2	3.47	7.14	1.51
10(1)_pt3	24.6	62.19	13.21	10(1)_pt3	2.22	2.39	1.05
10(2)_pt1	27.39	63.65	8.96	10(2)_pt1	2.53	5.3	1.07
10(2)_pt2	25.16	60.9	13.94	10(2)_pt2	2.29	2.49	1.14
10(2)_pt3	24.31	63.32	12.37	10(2)_pt3	2.16	4.52	1.02
10(2)_pt4	28.05	59.06	12.89	10(2)_pt4	1.85	1.98	1.29
10(2)_pt5	24.17	61.08	14.75	10(2)_pt5	1.33	1.48	0.94
10(2)_pt6	29.04	59.3	11.67	10(2)_pt6	1.97	2.14	0.93
10(2)_pt7	23.24	61.47	15.29	10(2)_pt7	1.56	3.52	1.14
10(2)_pt8	24.21	59.62	16.17	10(2)_pt8	2.25	2.23	1.16
10(3)_pt1	30.57	55.29	14.14	10(3)_pt1	4.59	5.63	1.16
10(3)_pt2	23.55	66.51	9.94	10(3)_pt2	3.84	7.95	1.94
10(3)_pt4	30.16	61.56	8.29	10(3)_pt4	2.78	3.02	1.2
10(3)_pt5	28.27	61.6	10.14	10(3)_pt5	1.82	2.2	0.57
10(3)_pt6	28.18	58.59	13.23	10(3)_pt6	2.39	2.56	1.13
10(3)_pt7	26.43	59.15	14.41	10(3)_pt7	1.44	1.57	0.69
10(3)_pt8	30.97	56.21	12.82	10(3)_pt8	2.72	1.68	0.92
Average:	26.70	60.89	12.41		2.38	3.31	1.09

b) $(\text{Bi}_x\text{Sb}_{1-x})_2\text{Te}_3$ with $x = 0.5$

Philips/FEI CM300 UT FEG; 300 keV acc. Voltage; Thermo Noran NSS Ge-Detector (yellow cell color)

Philips/FEI CM30 T Lab₆; 300 keV acc. Voltage; Thermo Noran NSS Si(Li)-Detector (white cell color)

<i>Atom%</i>	<i>Sb-L</i>	<i>Te-L</i>	<i>Bi-L</i>	<i>esd</i>	<i>Sb-L</i>	<i>Te-L</i>	<i>Bi-L</i>
01(1)_pt1	16.73	56.46	26.81	01(1)_pt1	2	4.27	1.46
01(1)_pt2	15.43	62.01	22.56	01(1)_pt2	0.92	1.02	0.84
01(1)_pt3	15.25	61.13	23.63	01(1)_pt3	0.89	2.17	0.66
01(1)_pt4	14.01	61.97	24.02	01(1)_pt4	2.28	2.27	2.23
01(2)_pt1	16.03	58.31	25.66	01(2)_pt1	1.91	4	1.33
01(2)_pt2	16.07	60.58	23.34	01(2)_pt2	1.33	1.31	1.01
01(2)_pt3	16.6	59.8	23.6	01(2)_pt3	1.57	1.57	1.17
01(2)_pt4	16.87	60.65	22.48	01(2)_pt4	1.83	1.82	1.28
01(2)_pt6	16.81	60.2	22.99	01(2)_pt6	1.82	1.8	1.31
01(3)_pt1	17.12	59.27	23.61	01(3)_pt1	1.14	1.15	0.88
01(3)_pt2	16.28	58.65	25.07	01(3)_pt2	1.61	0.97	0.63
01(3)_pt3	16.39	60.57	23.04	01(3)_pt3	1.38	1.71	0.63
01(3)_pt4	17	59.51	23.5	01(3)_pt4	1.3	1.61	0.59

<i>01(3)_pt5</i>	15.53	57.48	26.98
<i>01(3)_pt6</i>	16.34	59.6	24.06
<i>1(1)_pt1</i>	14.78	61.97	23.25
<i>1(1)_pt2</i>	15.76	59.92	24.32
<i>1(1)_pt3</i>	14.05	63.11	22.84
<i>1(1)_pt4</i>	34.87	47.39	17.75
<i>1(1)_pt5</i>	16.75	61.4	21.85
<i>1(2)_pt1</i>	20.08	62.13	17.8
<i>1(2)_pt3</i>	18.5	58.65	22.86
<i>1(2)_pt4</i>	16.18	64.99	18.82
<i>1(2)_pt5</i>	17.71	60.25	22.03
<i>1(3)_pt1</i>	14.55	63.74	21.71
<i>1(3)_pt2</i>	14.34	64.87	20.79
Average:	16.92	60.18	22.90

<i>01(3)_pt5</i>	1.24	2.66	1.18
<i>01(3)_pt6</i>	0.61	0.67	0.47
<i>1(1)_pt1</i>	1.59	3.67	1.41
<i>1(1)_pt2</i>	2.72	3.23	1.24
<i>1(1)_pt3</i>	2.57	5.54	1.55
<i>1(1)_pt4</i>	2.43	2.83	0.94
<i>1(1)_pt5</i>	1.3	2.77	1.07
<i>1(2)_pt1</i>	2.01	4.29	1.11
<i>1(2)_pt3</i>	2.47	2.93	1.08
<i>1(2)_pt4</i>	1.97	2.07	1.14
<i>1(2)_pt5</i>	2.64	3.16	1.18
<i>1(3)_pt1</i>	2.83	5.97	1.74
<i>1(3)_pt2</i>	1.73	3.63	1.04
	1.77	2.66	1.12

c) $(\text{Bi}_x\text{Sb}_{1-x})_2\text{Te}_3$ with $x = 0.75$

Philips/FEI CM300 UT FEG; 300 keV acc. Voltage; Thermo Noran NSS Ge-Detector

Atom%	Sb-L	Te-L	Bi-L
<i>11(1)_pt1</i>	6.63	57.99	35.37
<i>11(1)_pt2</i>	4.61	59.22	36.17
<i>11(1)_pt3</i>	8.43	59.81	31.76
<i>11(1)_pt4</i>	8.93	59.8	31.27
<i>11(3)_pt1</i>	9.31	62.02	28.68
<i>11(3)_pt2</i>	6.97	59.86	33.17
<i>11(3)_pt3</i>	6.08	61.08	32.84
<i>11(4)_pt2</i>	10.44	56.9	32.66
<i>11(4)_pt3</i>	5.9	61.37	32.73
Average:	7.48	59.78	32.74

esd	Sb-L	Te-L	Bi-L
<i>11(1)_pt1</i>	1.34	2.92	1.48
<i>11(1)_pt2</i>	1.35	2.92	1.47
<i>11(1)_pt3</i>	1.22	2.63	1.26
<i>11(1)_pt4</i>	2.6	2.66	2.74
<i>11(3)_pt1</i>	2.28	4.88	2.3
<i>11(3)_pt2</i>	1.57	3.4	1.64
<i>11(3)_pt3</i>	1.46	3.18	1.62
<i>11(4)_pt2</i>	1.47	1.56	1.62
<i>11(4)_pt3</i>	1.89	4.03	2.01
	1.69	3.13	1.79